A First look at NGRIP Surface Climatology (1997-2001) using Automatic Weather Station Data

Jason E. Box
Byrd Polar Research Center
The Ohio State University, Columbus, Ohio, USA.
box.11@osu.edu

Contents

1   Introduction

Greenland ice sheet automatic weather station (AWS) data provide high temporal resolution climate information for NGRIP (75.0998° N, 42.3326 W, 2918 m), where a tremendously long ice core climate record is becoming available (Johnsen et al, 2001; Gunderstrup et al., 2001). In this paper, an overview is made of the surface climatology of NGRIP to support work on ice core interpretation using NGRIP meteorological observations and snow pits. Valuable perspective is given by comparison of NGRIP climate with other deep ice core sites (Summit and Camp Century), where AWS data are also available.

2   Data

Beginning in 1995, automatic weather stations have been installed on the Greenland ice sheet as part of NASA's PARCA program (Thomas et al. 2001, Steffen et al. 1996). Between 1 and 5 stations have been added to the network since 1995. Presently, the Greenland Climate Network (GC-Net) consists of 20 stations distributed widely over Greenland's inland ice (**Figure 1**). The system samples 27 surface climate parameters on minute time-scales (Table 1, **Figure 2**), averages, stores, and transmits the hourly data via GOES and ARGOS communication satellites. All data have been quality checked by visual inspection and filtered using statistical methods (Steffen and Box, 2001). Prior to year 2000 maintenance visits, a software problem led to missing temperature measurements below -51° C. A temperature proxy based on the humidity instrument response made possible

estimation of temperatures between -50° C and -60° C. Below -60°C, data are missing before mid 2000. Wind speed measurements have been interrupted, in some cases as long as 2 months, caused by frost growth on wind sensors. The combined wind speed and direction record include 32% missing data due to frost. Frost has led to data gaps in other measured parameters, such as: surface height, solar and net radiation.

Additional meteorological data are available from the GEUS AWS running at NGRIP from mid 1997 to mid 2001 (Carl Bøggild, ceb@geus.dk). The GEUS tower was situated ~100 m from the NASA AWS. Co-analysis of the GEUS data promises to give valuable insight into spatial variance in ice sheet meteorology and also makes possible the filling of occasional data gaps. The GEUS tower was equipped with an instrument that measures downwelling thermal radiation, a key tool to perform cloud climatology.
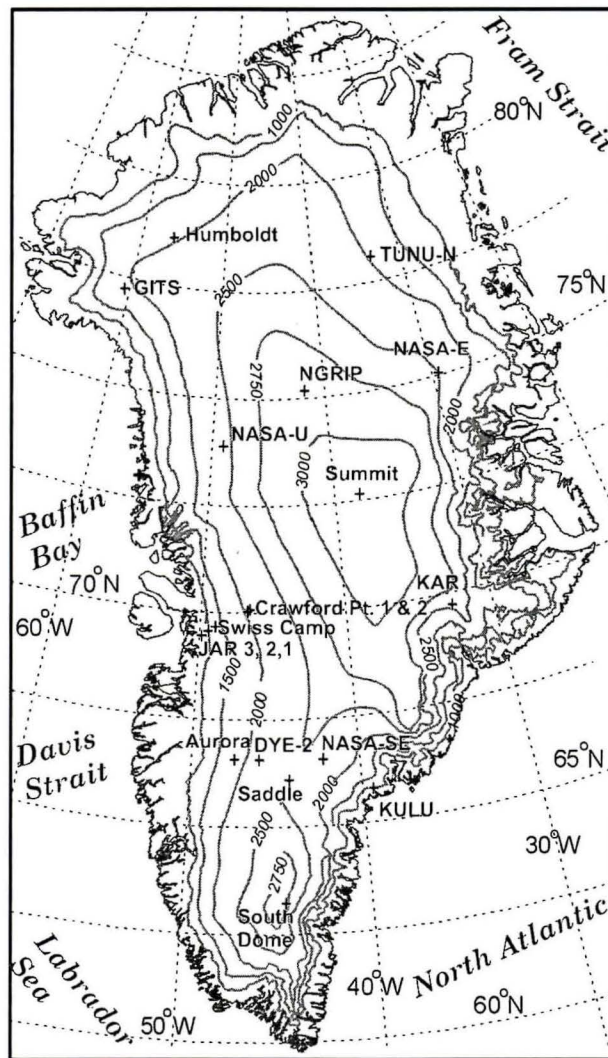

Figure 1. Location map of Greenland Climate Network Sites, including NGRIP
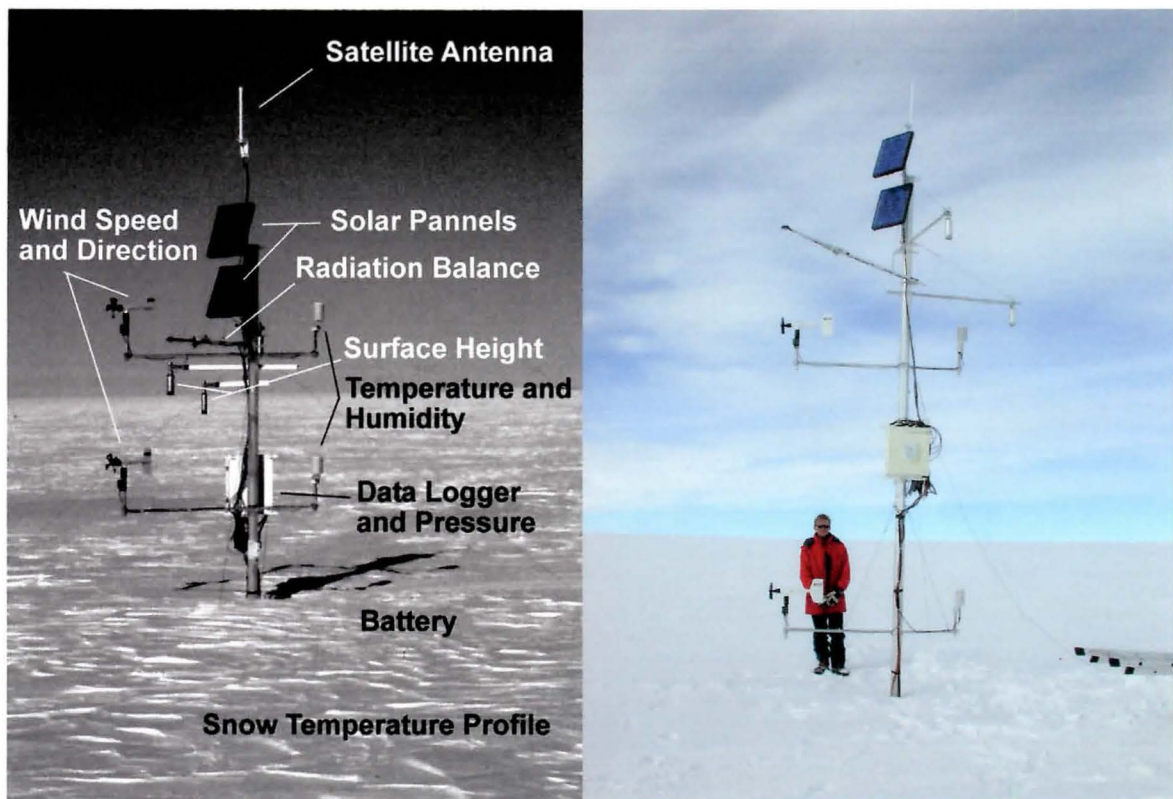
Figure 2. (left) Photo of a GC-Net AWS featuring instrumentation. (right) In 2001, NGRIP field workers aided AWS maintenance.

Table 1. GC-Net Instruments Employed in this Study

Parameter	Instrument	Approximate Uncertainty	Sampling Rate
Downwelling Shortwave	LI-COR 200SZ	5%	15 s
Upwelling Shortwave	LI-COR 200SZ	10%	15 s
Net Radiation	REBS Q*7	20%	15 s
Air Temperature	Vaisala 50YC	0.1 °C	60 s
Air Temperature	Type-E Thermocouple	0.1 °C.	15 s
Relative humidity	Vaisala INTERCAP or Vaisala HUMICAP 180	5% < 90% RH 3% > 90% RH	60 s
Surface height change	Campbell Sci. SR-50	1 mm	10 min
Multiplexer	Campbell Sci. AM-25T	-	-
Data logger	Campbell Sci. CR-10/10X	-	-

3 NGRIP Surface Climatology Based on AWS Data

This section begins with a climatological overview of individual parameters, such as temperature, wind speed and direction, giving a broad description of the present surface climate and mentioning some interesting features in the data. The section includes examples of applications of the AWS data to more detailed and holistic climatologies such as the surface energy balance, sublimation, and blowing snow.

3.1 Air Temperature

Annual average temperatures for NGRIP and Summit are summarized in Table 2. The values at NGRIP are very close in magnitude to those of Summit (a.k.a. GISP2) (72.5794 °N, 38.5042 °W, 3208 m), despite the fact that NGRIP is 290 m lower in elevation (Table 2). NGRIP is 303 km north northwest of Summit (2.5 ° latitude or 280 km further north). The difference in latitude accounts for the lower temperature commonly observed at NGRIP (Steffen and Box, 2001). February is the coldest month at NGRIP (-45 °C). July is the warmest month (-11 °C). Temperatures are both slightly colder in winter and warmer in summer at NGRIP as compared to Summit. In other words, the amplitude of the monthly mean annual cycle in temperature is 33.7 °C at NGRIP, as compared to 30.6 °C at Summit. The temperature difference between NGRIP and lower elevation sites is greater in winter than in summer, owing to the tighter pressure (and atmospheric circulation) distribution over the Arctic in winter (Serreze et al. 1993). The record low hourly average temperature observed at all GC-Net AWS sites (-67 °C) occurred at NGRIP, 1800 UTC on the 3rd of February, 2002. Such cold conditions are caused by an extended period of low wind speeds and high pressure, indicative of the clear sky conditions that lead to prolonged surface radiative cooling and sinking temperatures. During this extremely cold period, the air temperature sensors indicated a value of -67.1 °C at ~2 m above the surface and -66.4 C at ~3.2 m height. The vertical temperature inversion suggests a snow surface temperature of approximately –70° C. This value is within a few degrees of the record low temperature for the northern hemisphere, set in the topographic sinks of Siberia.

Table 2. Annual Mean Temperatures [°C] at NGRIP and Summit

Year	NGRIP 2m	Summit 2 m	NGRIP -10 m firn	Summit -10 m firn
1997	*	-29.5	*	-31.1
1998	-28.9	-27.8	-29.7	*
1999	-28.9	-27.8	-29.5	-31.1
2000	-29.5	-30.2	-31.7	-31.3
2001	-28.7	-28.9	-31.6	-31.2

* - insufficient data

The NGRIP vertical temperature gradient near the surface is indicative of a temperature inversion, i.e. temperature increases with height above the surface, up to ~100 m. A surface temperature inversion is observed 80% of the time at NGRIP (Box and Steffen, 2001). Buoyant instability conditions (opposite of temperature inversion, buoyant stability) are occasionally observed at midday in summer, when the surface is heated by absorption of solar radiation above the temperature of the air in the few meters above the surface. Given some wind, unstable conditions cause a turbulent flux of heat, water vapor, and chemical isotopes away from the surface. The predominant case at NGRIP, however, is of a temperature gradient that drives a flux toward the surface. There are sufficient AWS data to make detailed models of vertical chemical fluxes. The application to water vapor appears in Box (2001) and Box and Steffen (2001). Sublimation is discussed further in section 3.9.

3.2   Firn Temperatures

Monthly mean firn temperatures are calculated for constant depths using the raw firn temperature profile data and surface height change measurements. The amplitude of the annual firn temperature variation decreases with increasing depth and includes a phase shift of the annual cycle, given that the thermal wave takes time top penetrate the firn (**Figure 3**). Near a depth of 10 m, the temperature wave is out of phase with the surface air temperature. Thus it takes ~1 year for a thermal perturbation to conduct to 10 m in the firn. The 10 m temperature has been used extensively in the literature as a proxy for the annual mean temperature, e.g. Benson, 1962. However, a thermal cycle still exists at 10 m (and well below 10 m). Furthermore, the depth at which the temperature wave is exactly out of phase with the surface would depend on the firn density, porosity, and other ice properties that control the thermal conductivity. Thus, 10 m is not a critical depth for measuring annual mean temperature. As the firn temperature string got deeper with time, owing to net annual snow accumulation, it became impossible to calculate the −1 m temperature by interpolation between individual thermocouple measurements, but it then became possible to calculate the −10 m temperature. The 0 m surface temperature is calculated by extrapolation of the observed air temperature profile. The average 9 m firn temperature (1997-2001) has been computed to be -31.62 °C, and indicates a -0.51 °C trend over 4 years. Some other firn temperature statistics are given in **Table 2**. Annual average firn temperature is somewhat lower than air temperature, values owing to the fact that air temperature are affected by the persistent temperature inversion, and average air temperature measurements are very slightly affected by a positive bias from solar overheating of the instruments in summer.
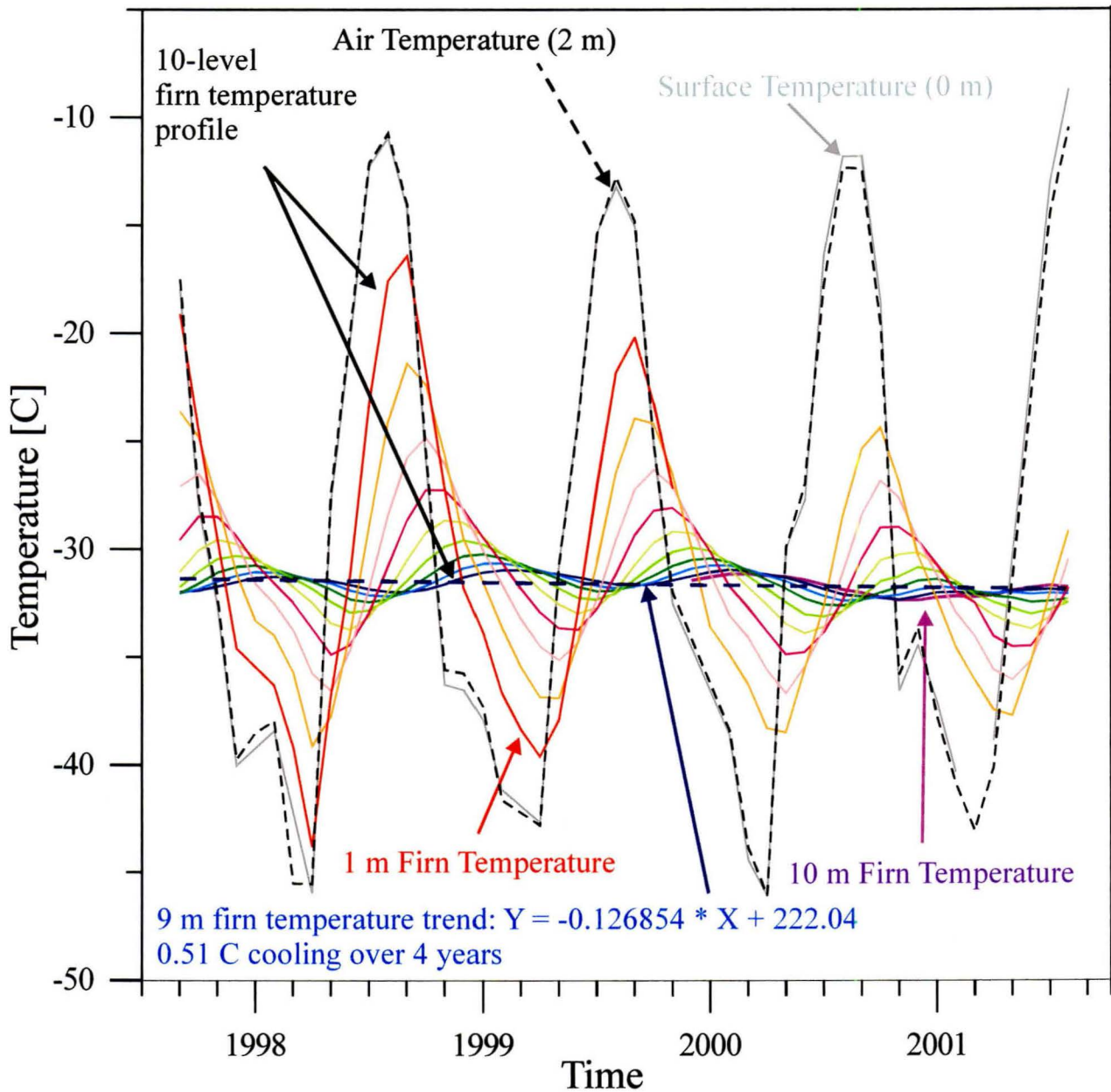
Figure 3. 48 monthly air, surface, and firn temperature measurements from NGRIP between August 1997 and July 2001.

3.3 Humidity

The average concentration of atmospheric water vapor at NGRIP was 0.69 g m^{-3} in 2000. Maximum monthly values are observed in July (1.88 g m^{-3}) and August (1.97 g m^{-3}). Minimum monthly values are observed in February (0.075 g m^{-3}). There are few places at the surface of the earth with humidity concentrations so low as they are in winter at high elevations over ice sheets. At NGRIP, the vertical gradient of water vapor concentration between 1 m and 2 m above the surface is typically positive, indicating the potential for a flux of water vapor from the atmosphere to the surface. This is in contrast to lower elevation regions of the ice sheet, where there is commonly a

water vapor gradient directed away from the surface. The range of monthly average vertical specific humidity gradient is between 0.066 g m^{-3} m^{-1} (deposition) and –0.115 g m^{-3} m^{-1} (sublimation). Net annual vertical water vapor gradients result in a gain of mass by the surface of 32 mm w e y^{-1} (Box and Steffen, 2001). The interannual variability in vertical water vapor exchange is about ±15 mm y^{-1}. Given the small accumulation rate at NGRIP of ~180 mm w e y^{-1}, water vapor deposition represents a significant component of the surface mass balance.

3.4   Wind Speed and Direction

Wind speeds at NGRIP are commonly low (4.1 m s^{-1} annual average) as compared to lower elevation sites (7.1 m s^{-1} at equilibrium line altitude, Swiss Camp) (Steffen and Box, 2001). At NGRIP, there is a prevailing wind direction which is apparently katabatic. The wind direction frequency peak corresponds nearly with the upslope direction (Figure 4). The difference between the prevailing wind direction (180°) and slope direction (~160°) is probably due to the Coriolis effect (Bromwich et al. 1996), which turns large scale flow to the right in the northern hemisphere. Figure 4 indicates a small trend to more southerly wind directions as the wind speed increases. This is consistent with observations of storms at lower elevation sites in western Greenland. Storms typically have a more southerly component than the prevailing wind direction. This is also influenced by the Coriolis effect, which depends on the wind speed, among other things such as the latitude and the rotation rate of the planet.
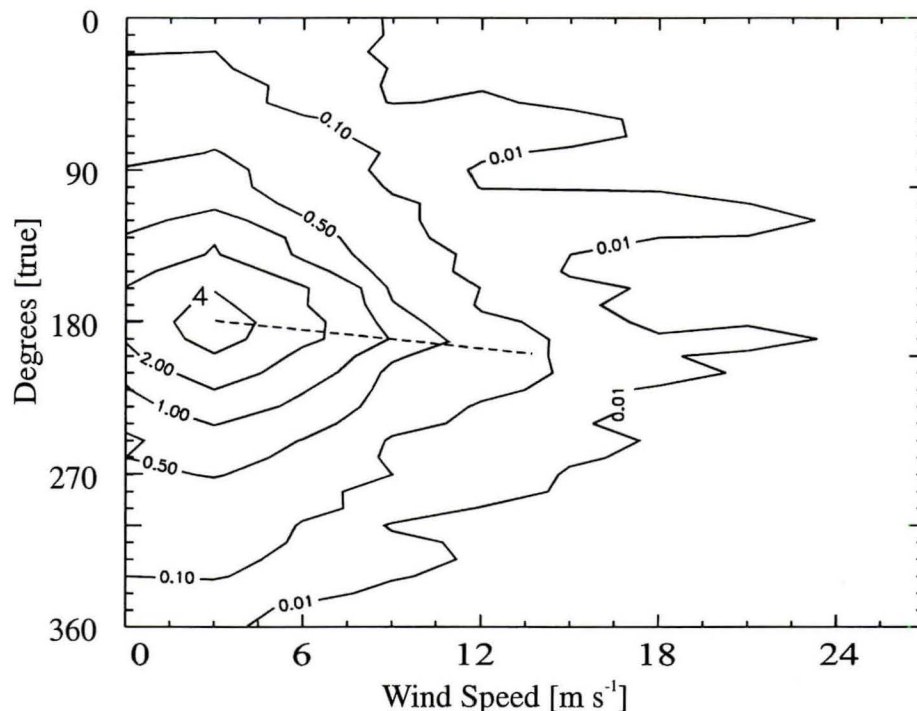

Figure 4. Nomogram of wind speed and direction from 4 years of NGRIP AWS data including a dashed line that indicates a wind direction trend as wind speed increases.

3.5   Accumulation Rates

GC-Net AWS are equipped with two sonic ranging instruments to sample surface height variations at 10 minute intervals. These data make possible to examination of individual snow events and to derive year to year variations in accumulation rate. The annual record of daily average surface height change is shorn in Figure 5. A linear model for accumulation fits these data very well, with residual 1 standard deviation of ±0.04 m. The assumption that accumulation is uniform through the year is valid for NGRIP and Summit. At other GC-Net sites, such as South Dome in the south, there is a winter accumulation peak. In northwestern Greenland, there is a summer accumulation peak (Steffen and Box, 2001). At NGRIP, snowfall events are relatively small. There are only 4 distinct snow events over 4 years of observations that exceed 4 cm. Looking at the remainder of time, accumulation appears to occur at a slow continuous rate (same at Summit). Nighttime deposition of rime frost on the surface is a common observation at ice sheet plateau sites, such as NGRIP and Summit (personal observation), and dome Fujii, Antarctica (Kameda, 1997). This is and clear-shy ice crystal precipitation are the proposed accumulation mechanisms at high elevations in Greenland.
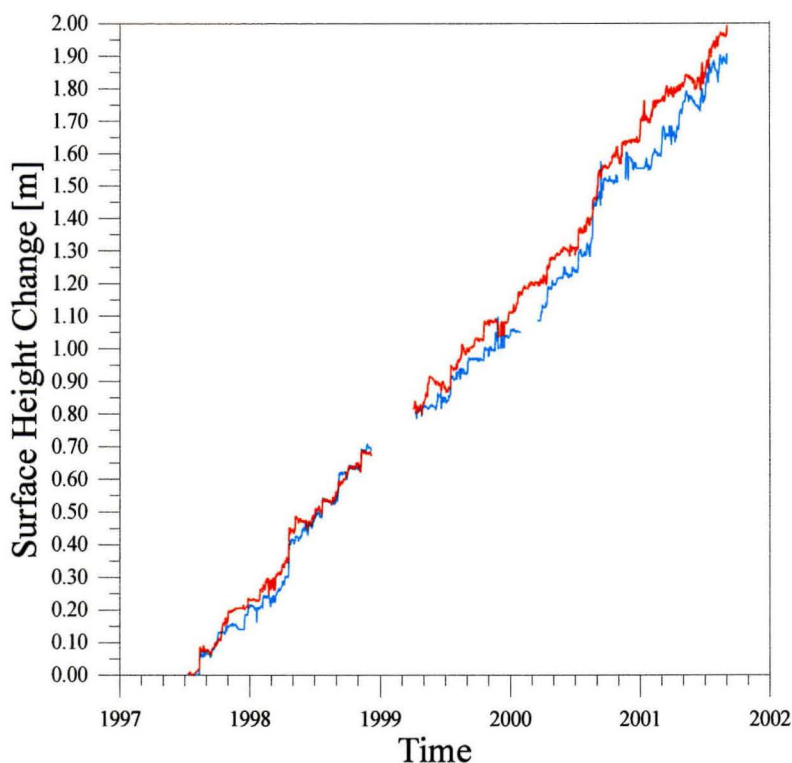

Figure 5. Daily average surface height changes at the NGRIP AWS 1997-2001

Snow pits were dug by J. Box and K. Daniels during the 2000 site visit using a 500 cm^{-3} 'Kelly Cutter'. The density profiles are summarized in **Table 3**. Y. Fujii made a detailed drawing of the snow pit stratigraphy (**Figure 6**). One impression from the NGRIP snow pits was the high degree of smoothness in the layering over the ~1.5 m width of the drawing. The smooth layering is due to the

relatively low wind speeds observed at NGRIP. A thick homogeneous layer is observed to have occurred in early 1998, visible in surface height and snow pit data (**Figure 5**, **Figure 6**). Hard surface horizons in mid 1997 and 1999 are probably caused by compaction of the surface by people and vehicles. In 1997, a snow cat hydraulic arm was used to install the weather station. In 1999, it appears that AWS visitors trampled the surface where the pit was eventually dug. Therefore, more care must be taken in the future visiting the AWS not to disturb the surface and to select sites for snow pits where the surface is undisturbed.
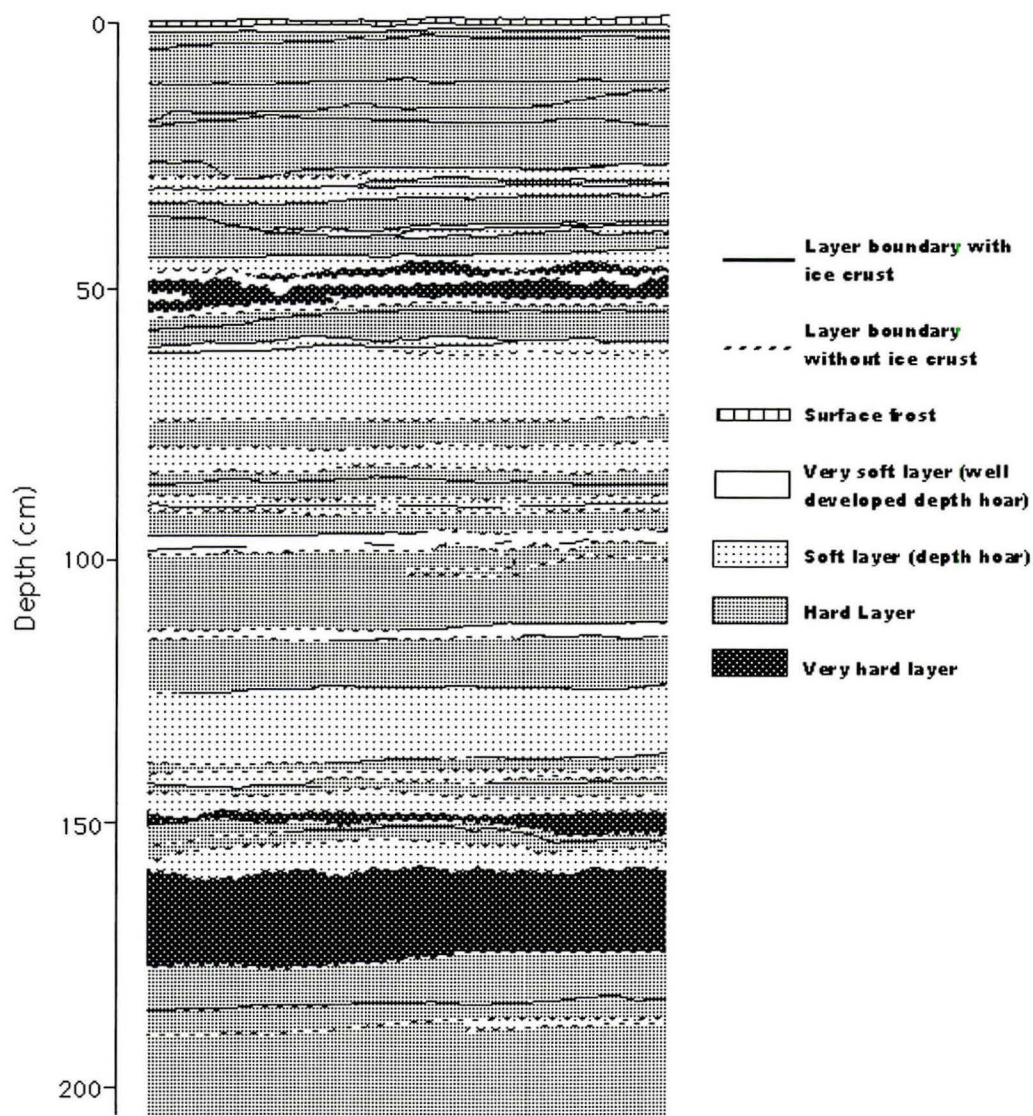

Figure 6. Drawing of NGRIP 2000 snow pit (same pit as **Table 3.**) by Y. Fujii (fujii@pmg.nipr.ac.jp).

Table 3. Snow density profiles at NGRIP

Depth (cm)	Run 1: 17 June 2001 (kg m^{-3})	Run 2: 18 June 2001 (kg m^{-3})
0-10	288	300
10-20	295	303
20-30	332	322
30-40	307	315
40-50	293	298
50-60	313	300
60-70	343	320
70-80	328	320
80-90	321	313
90-100	283	285
100-110	350	332
110-120	326	335
120-130	366	352
130-140	314	322
140-150	309	326
150-160	315	335
160-170	417	355
170-180	341	384
180-190	-	355
190-200	-	347
200-210	-	366

3.6 Pressure

Lower pressures are observed in winter than in summer (**Figure** 7). Interdiurnal fluctuations sometime exceed 30 hPa. Winter atmospheric circulation is more vigorous, resulting in greater winter variability in temperature, wind speed, and wind direction. The large changes in pressure have been shown to signify abrupt changes in temperature, including the abrupt spring temperature rise (Rogers et al. 1997). The amplitude of the annual cycle of monthly means is 26.7 hPa, slightly larger than at Summit. Interannual variability in pressure serves as an indicator of the intensity of cyclonic activity from one year to the next. Annual average pressure was 692.9 hPa in 1998, 689.3 hPa in 1999, 690.7 hPa in 2000, and 691.1 hPa in 2001. The higher pressures in 1998 and 2001 are probably linked with the warmer temperatures observed in those years, owing to more clear sky conditions in summer. Further investigation here is necessary for more conclusive results.
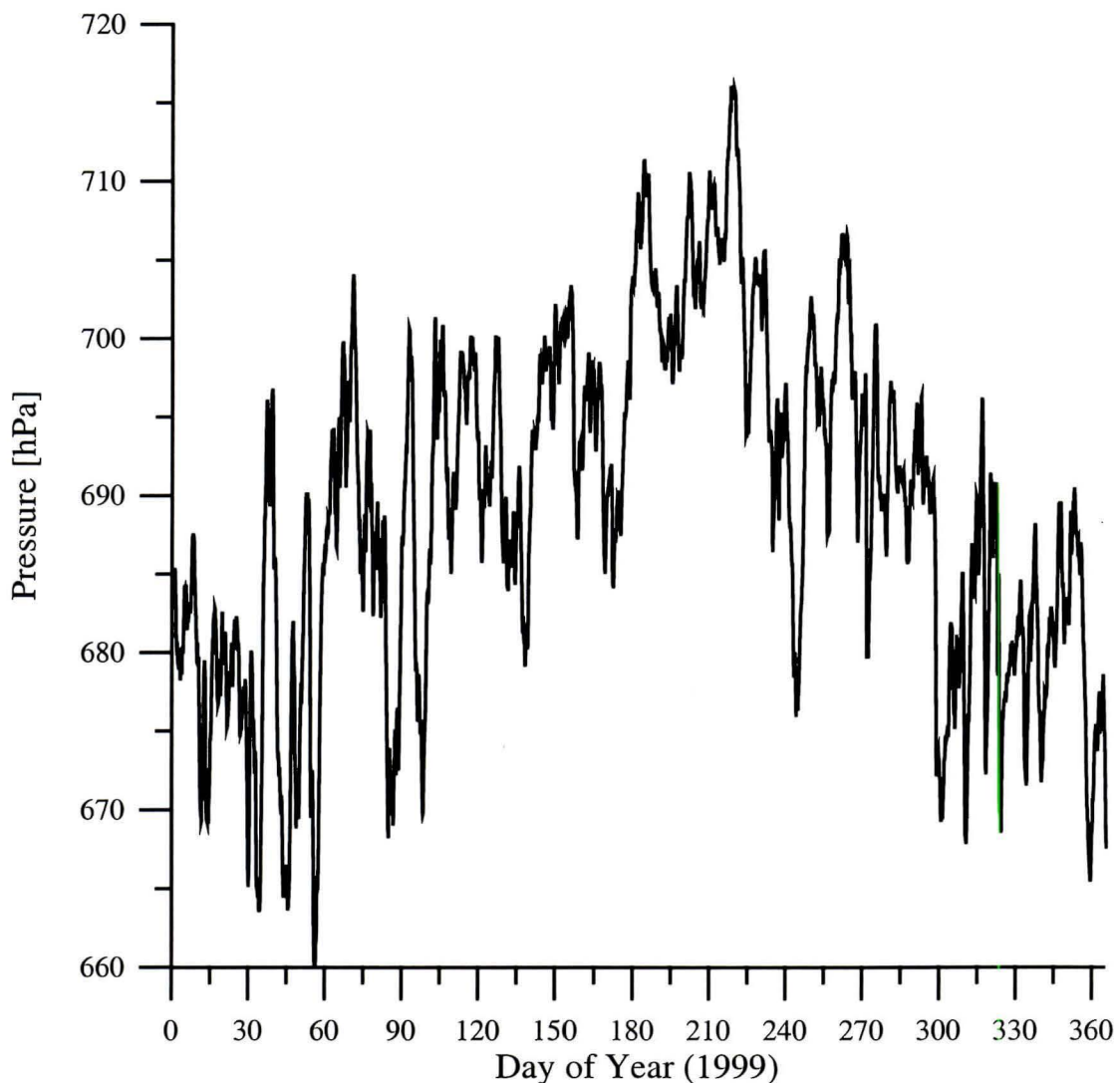

Figure 7. Annual pattern of hourly surface pressure at NGRIP in 1999

11

3.7 Blowing Snow

Annual blowing snow transport (Q_{act}), in metric tons per meter perpendicular to the wind, has been estimated to be 120 t m^{-1} y^{-1} (Box, 2001) by the model proposed by Tabler (1991) (Table 4). Blowing snow transport at NGRIP is relatively small, as compared to lower elevation sites, which exhibit stronger katabatic winds. The proportion of snowfall relocated by the wind (θ) at NGRIP is about 60%. θ is calculated as the ratio of the cumulative negative and positive surface height changes over the course of a year and is corrected for firn compaction. Other variables given in **Table 4** are: potential blowing snow transport (Q_{pot}) assuming unlimited snow supply; precipitation from atmospheric modeling (P) (Bromwich et al. 2001); blowing snow sublimation (Q_{evap}) derived assuming the majority of transported snow sublimates; the implied accumulation (i.e. P-Q_{evap}); AWS derived accumulation uses the slope of surface height change over the year times the number of samples per year (8760 hours) and is corrected for compaction (see Box, 2001); the maximum transport distance of blowing snow (R_μ) (see Box, 2001, Chapter 9); and the number of snow events detected using a 3 cm threshold of daily average surface height measurements.

Table 4. Blowing Snow Statistics for Select Ice Sheet Locations

Site	Year	Q_{pot} t m^{-1} y^{-1}	Q_{act} t m^{-1} y^{-1}	P mm y^{-1}	θ	Q_{evap} mm y^{-1}	Implied Accum. mm y^{-1}	AWS derived Accum. mm y^{-1}	R_μ	N. of Snow Events y^{-1} > 3 cm
GITS (a.k.a. Camp Century)	1996	701	313	344	0.45	155	189	406	4045	33
Summit	1997	613	191	113	0.65	73	40	216	5200	22
South Dome	1998	1839	896	416	0.42	175	241	517	10252	25
NGRIP	1998	290	120	118	0.60	71	47	188	3402	16

3.8 Radiation Balance

Major components of the radiant energy balance at NGRIP are shown in **Figure 8** (Box et al, in preparation). In June, solar ('shortwave') radiation peaks, owing to seasonal solar declination variations. The surface reflects about 85% of the incident shortwave energy, absorbing up to 70 W m^{-2} on average in summer. Thermal infrared radiation ('longwave') fluxes peak one month later than solar visible radiation, owing to the fact that atmospheric and surface heating lag the solar input, as heat accumulates in the climate system. On average and throughout the year, surface emitted longwave exceeds the downwelling longwave flux, resulting in a negative thermal radiation balance. The sum of shortwave and longwave radiation fluxes is the 'net radiation'. In summer, net radiation is on average positive, as the absorbed shortwave radiation exceeds the net longwave flux, leading to surface heating. In winter, with little or no solar radiation input, the surface net radiation balance is

predominantly negative. A negative radiation balance leads to surface cooling and the development of the surface temperature inversion commonly observed over snow and ice surfaces. In some cases, clouds may induce a positive thermal radiation balance and positive net radiation, which has a warming effect on the surface. Positive net radiation often occurs at midday and negative net radiation occurs at night, leading to the daily cycle in temperature.
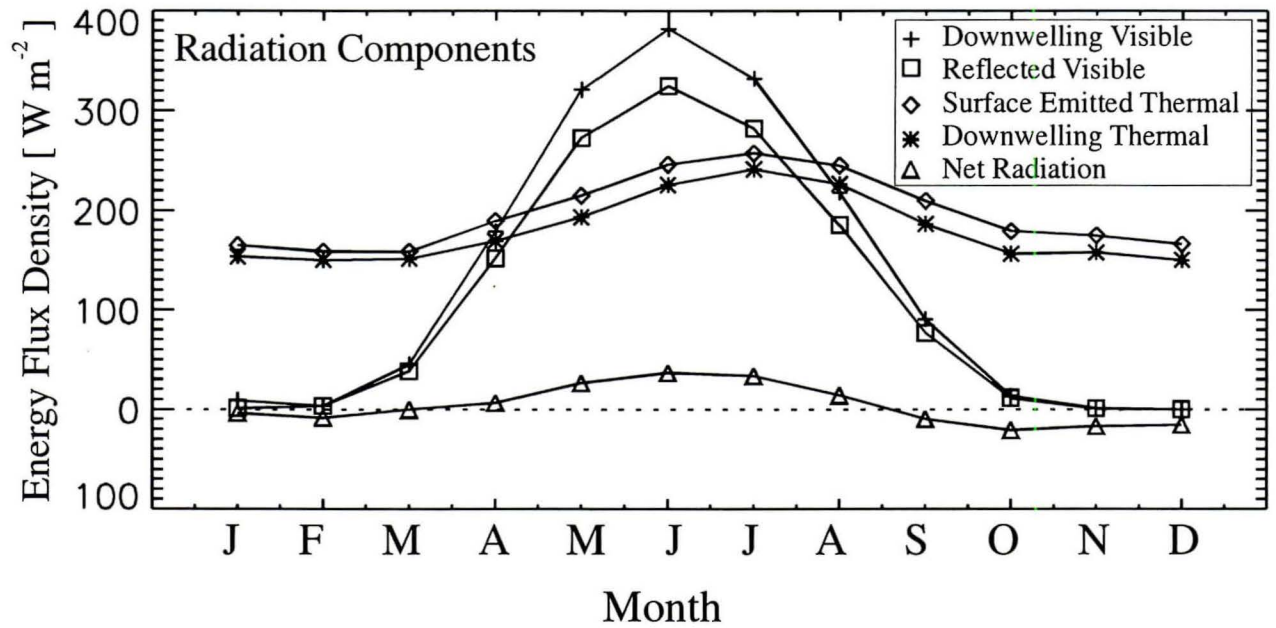

Figure 8. Surface radiation balance components at NGRIP based on in-situ observations and trend surface modeling.

3.9   Energy Balance

The surface energy balance is calculated using methods in Box and Steffen (2001), Box (2001), Box et al. (in preparation) and Oke (1987). Individual energy balance components are now discussed. At NGRIP, the sensible heat flux (Q_H) indicates a loss of heat from the atmosphere to the surface, particularly in winter, when surface radiative cooling leads to a strong temperature inversion (**Figure 9**). With warm air overlying a colder surface, the flux of sensible heat is toward the surface. The latent heat flux (Q_E), associated with sublimation and deposition of water vapor, is a relatively small component of the energy balance at NGRIP. Q_E indicates a general water vapor loss in summer and gain in winter. The net water vapor balance at NGRIP is positive (Box and Steffen, 2001), similar to Dome Fujii, Antarctica (Kameda et al. 1997). The firn conductive heat flux (Q_G) indicates that the near surface firn looses heat in winter and gains heat in summer. Q_G in the upper 1 m is very small, with monthly values on the order of 1-2 W m^{-2}. The net annual conductive flux is–0.1 W m^{-2} (Table 5). The residual of the energy balance (Q_M) is the combination error, stored heat, and energy of melting. Given that there is little or no surface melting at NGRIP and that the stored heat cannot be more than a few W m^{-2}, Q_M here indicates a substantial error in energy balance closure. The net radiation (Q^*) for NGRIP is probably too high, probably not because the surface albedo $(\alpha = 85\%)$ is too low, but that the downwelling shortwave $(S\downarrow)$ estimate is too high, or more likely that the downwelling longwave $(L\downarrow)$ is in error, i.e. too large in summer and the surface emitted longwave $(L\uparrow)$ is too low. Further development of the trend surface model or pursuing another energy balance model would eventually result in lower residual error.
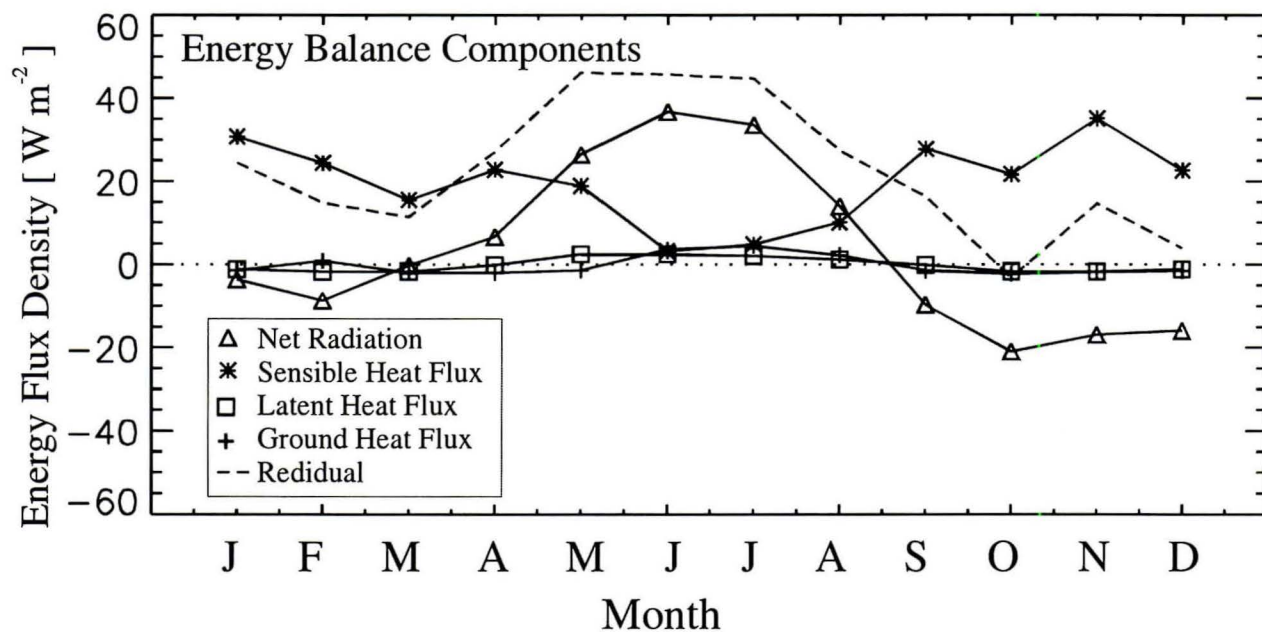

Figure 9. Surface energy balance components at NGRIP based on in-situ observations and trend surface modeling.

Table 5. Average energy balance components at NGRIP (1997-2001) based on trend surface modeling of GC-Net data

	S↓	S↑	L↓	L↑	Q*	α	Q_H	Q_E	Q_G	Q_M
Jan	9	1	154	165	-4	85	31	-1.5	-1.2	24
Feb	3	4	150	159	-9	85	24	0.8	-1.7	15
Mar	45	38	151	159	0	85	15	-2.0	-1.7	11
Apr	179	152	169	189	7	85	23	-2.1	-0.2	27
May	321	273	193	215	26	85	19	-1.5	2.4	46
Jun	382	325	226	246	37	85	3	3.5	2.4	46
Jul	332	282	241	257	34	85	5	4.5	2.0	45
Aug	218	185	226	245	14	85	10	2.2	1.1	27
Sep	90	77	186	210	-10	85	28	-1.6	-0.2	16
Oct	13	11	156	179	-21	85	22	-2.3	-1.7	-3
Nov	1	1	158	175	-17	85	35	-1.9	-1.7	15
Dec	0	0	150	166	-16	85	23	-1.6	-1.2	4
Average	133	112	180	197	3	85	20	-0.3	-0.1	23

4 Concluding Remarks

This paper represents a first look into the presently 5-year long NGRIP AWS record (1997-2002). There are many interesting aspects of the data that should be pursued further. A long term goal should be to reconcile the short-duration high temporal resolution information from the AWS with the long-duration lower temporal resolution ice core data. The bridge between these two datasets may lie in the snow pit data that has been collected. Thus, more effort should go into correlating the weather data time series from the AWS with detailed snow pit data. This is challenging, given the low accumulation rate at NGRIP and the fact that the snow events are small. Nevertheless, the data exist to make a clearer picture of the transfer of the weather information into the ice core. It is a matter of looking more into the data and joining datasets gathered by different investigators.

5 Acknowledgements

6 References

Benson, C. S., Stratigraphic Studies in the Snow and Firn on the Greenland Ice Sheet, *U.S. Army SIPRE Research Report,* Vol. 70 CRREL, pp. 93, 1962.

Box, J. E. and K. Steffen, Sublimation estimates for the Greenland ice sheet using automated weather station observations, *J. Geophys. Res.,* 106(D24), 33965-33982, 2001.

Box, J. E., Surface Water Vapor Exchanges on the Greenland Ice Sheet Derived from Automated Weather Station Data, PhD Thesis, Department of Geography, University of Colorado, Boulder, CO, Cooperative Institute for Research in Environmental Sciences, 190 pp, 2001. *http://cires.colorado.edu/people/steffen.group/jbox/PhD/J_Box_PhD_Thesis_2001.pdf*

Box, J. E., K. Steffen, N. Cullen, Greenland Ice Sheet Broadband Radiation Components Based on In-situ Data, in preparation for submission to *J. Applied Meteorology.*

Bromwich, D. H, Chen, Qui-shi, Bai, Le-sheng, Cassano, E., N., Li, Yufang, Modeled precipitation variability over the Greenland ice sheet, J. Geophys. Res. Vol. 106(D24), 33,891-33,8908, 2001.

Bromwich, D.H., Y. Du, and K.M. Hines. Wintertime Surface Winds over the Greenland Ice Sheet. Mon. Wea. Rev., 124, 1941-1947, 1996.

Gundestrup, N., NGRIP Field Season Report 2001, Dept. Geophysics, Copenhagen University, 143 pp, 2001.

Johnsen Sigfus J., D. Dahl-Jensen, N. Gundestrup, J. P. Steffensen, H. B. Clausen, H. Miller, V. Masson-Delmotte, A. E. Sveinbjörnsdottir, J. White, Oxygen isotope and palaeotemperature records from six Greenland ice-core stations: Camp Century, Dye-3, GRIP, GISP2, Renland and NorthGRIP, *Journal of Quaternary Science*, Vol. 16, p. 299-307, 2001

Kameda, T., Azuma, N., Furukawa, T., Ageta, Y. and Takahashi, S., Surface mass balance, sublimation and snow temperatures at Dome Fuji Station, Antarctica, in 1995, *Proceedings of the NIPR Symposium on Polar Meteorology and Glaciology*, Vol. 11 NIPR, Tokyo, Japan, 24-34, 1997.

Oke, T. R., Boundary layer climates, *Methuen & Co.*, 435 pp., 1987.

Rogers, J.C., R.A. Hellstrom, E. Mosley-Thompson, and C.-C. Wang, 1997: An abrupt spring air temperature rise over the Greenland ice cap. *J. Geophys. Res.*, 102(D12), 13,793-13,800.

Serreze, M. C., J. E. Box, R. G. Barry, Characteristics of Arctic Synoptic Activity, *Journal of Meteorology and Atmospheric Physics*, Vol. 51, pp. 147-164, 1993.

Steffen, K. and J. E. Box, Surface climatology of the Greenland ice sheet: Greenland Climate Network 1995-1999, *J. Geophys. Res.*, 106(D24), 33951-33964, 2001.

Steffen, K., J. E. Box, and W. Abdalati, Greenland Climate Network: GC-Net, US Army Cold Regions Reattach and Engineering (CRREL), *CRREL monograph*, trib. to M. Meier, 1996.

Tabler, R. D., Snow Transport as a Function of Wind Speed and Height, In Cold Regions 6th Int. Specialty Conference, TCCP/ASCEW. Lebanon, NH, 729-738., 1991.

Thomas, Robert H. and PARCA Investigators, PARCA 2001, Program for Arctic Regional Climate Assessment (PARCA): Goals, key findings, and future directions, *J. Geophys. Res.* Vol. 106(D24), 33,691-33,706, 2001.